Annex A

Techniques and Computer Codes for Rational Modelling of Frequency-Dependent Components and Subnetworks

Bjørn Gustavsen

A.1 Introduction

Several power system components, such as overhead lines, underground cables and power transformers, are characterized by strongly frequency-dependent effects in their behaviour. The accurate simulation of electromagnetic transients [1] requires us to take the frequency dependency into account. One way of modelling such components is by characterizing their behaviour in the frequency domain, followed by a model extraction procedure. The use of rational functions is an essential ingredient in such modelling as it leads to highly efficient time-domain simulations [2].

Since most difficulties in frequency-dependent modelling of overhead lines and underground cables have been overcome these days [3–5], this annex focuses on the modelling of terminal equivalents from tabulated data. Here, significant challenges remain. Typical applications include modelling of subnetworks by frequency-dependent network equivalents [6, 7] and high-frequency transformer modelling [8, 9]. We first list the rational fitting methods that have been traditionally applied within the power systems area, and we describe the basic steps for including a rational model in a circuit simulator. We next describe a very powerful method for 'fitting' a rational function to the data, known as vector fitting [10]. A perturbation method [11] is described, which is capable of enforcing passivity of the model, thereby guaranteeing the stability of time-domain simulations. We next describe a freely available computer implementation of the above methods. Finally, the application of the software is demonstrated for high-frequency modelling of a transformer starting from frequency sweep measurements.

Transient Analysis of Power Systems: Solution Techniques, Tools and Applications, First Edition.
Edited by Juan A. Martinez-Velasco.

A.2 Rational Functions

A rational function can in the frequency domain be expressed in alternative forms, including:

- Polynomial form, see (A.1)
- Pole-zero form, see (A.2)
- Pole-residue form, see (A.3)
- State-space form, see (A.4):

$$f(s) = \frac{a_0 + a_1 s + \cdots a_n s^N}{1 + b_1 s + \cdots b_n s^N} \tag{A.1}$$

$$f(s) = k \frac{\prod_{m=1}^{N} (s - z_m)}{\prod_{m=1}^{N} (s - a_m)} \tag{A.2}$$

$$f(s) = \sum_{m=1}^{N} \frac{r_m}{s - a_m} + r_0 \tag{A.3}$$

$$f(s) = \mathbf{c}^T (s\mathbf{I} - \mathbf{A})^{-1} \mathbf{b} + r_0 \tag{A.4}$$

The problem at hand is to calculate the rational function $f(s)$, such that it approximates a given frequency response $h(s)$ as closely as possible.

$$f(s) \cong h(s) \tag{A.5}$$

This process is often referred to as "fitting".

A.3 Time-Domain Simulation

The motivation for using rational functions is twofold. It allows direct transformation from the frequency domain into the time domain, and it leads to highly efficient simulations in the time domain via recursive convolution [2]. For instance, with the pole-residue form (A.3), each term leads directly to the exponential form (A.5) for the time-domain impulse response, and the convolution between the impulse response and an input can with a fixed time-step be expressed by the *recursive convolution* form (A.6) [12]. The formulation (A.6) can be interfaced to EMTP-type programs via a Norton equivalent, where the current source is updated in each time-step. An alternative procedure is to generate an *equivalent lumped circuit* in an EMTP-type netlist [6, 13]. The latter approach, however, often produces large circuits and is less efficient than the recursive convolution approach:

$$f(s) = \sum_{m=1}^{N} \frac{r_m}{s - a_m} \rightarrow f(t) = \sum_{m=1}^{N} r_m e^{a_m t} \tag{A.6a}$$

$$y(t) = f(t) * u(t) \rightarrow \begin{cases} x_n = \alpha x_{n-1} + u_{n-1} \\ y_n = \beta x_n + \gamma u_n \end{cases} \tag{A.6b}$$

A.4 Fitting Techniques

A.4.1 Polynomial Fitting

Rational fitting (A.5) can in principle be easily done via the polynomial form (A.1) by multiplying with the denominator. This leads to the following linear least-squares (LS) problem:

$$\left(1 + b_1 s + \cdots b_n s^N\right) h(s) \cong a_0 + a_1 s + \cdots a_n s^N \tag{A.7}$$

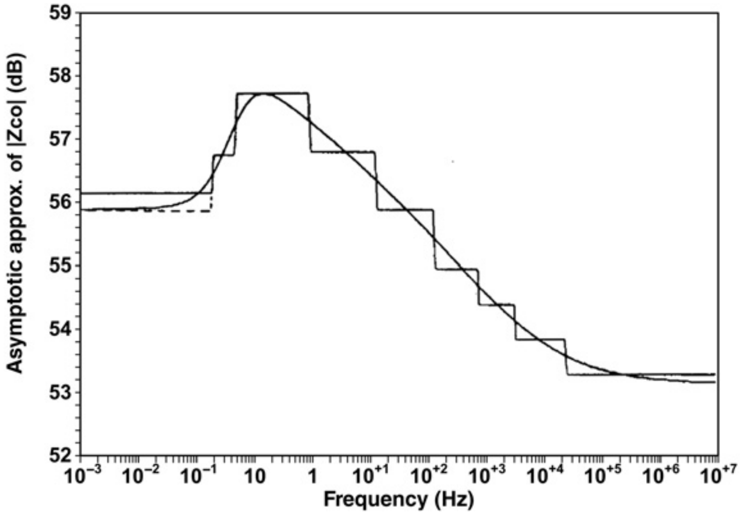

Figure A.1 J Martí fitting of rational function asymptotes to magnitude (Taken from [16]).

Direct solving of (A.7) leads to an approximation which is strongly biased. Although the biasing can be removed via reweighting (Sanathanan–Koerner iteration [14]), the method is troubled with effects of numerical ill-conditioning, which often limits its application to problems of low order and small bandwidths.

A.4.2 Bode's Asymptotic Fitting

In the case of frequency responses that are smooth and of minimum phase shift type, a quite accurate model can be obtained by fitting the magnitude function and using real poles and zeros in the left half-plane. This allows the fitting process to be based on the asymptotes of the rational function on the pole-zero form (A.2) [15]. The fitting process was automated by J.R. Martí [3] in 1982 for application to travelling-wave type transmission line modelling. Starting from a low frequency, a pole/zero is added when the asymptote departs by a positive/negative amount higher than a predefined tolerance – see Figure A.1. Finally, the zero locations are adjusted iteratively to improve the accuracy of the final result. The method has proved to be robust and usually sufficiently accurate. More importantly, it avoids the numerical problems associated with polynomial formulations. It is still in use in several EMTP-type programs for frequency-dependent modelling of transmission lines by the travelling wave method.

A.4.3 Vector Fitting

More general fitting approaches are those based on vector fitting (VF) [10]. These iterative methods are applicable to both smooth and non-smooth data as the fitter will automatically produce real and/or complex poles and residues as needed. VF relocates a set of initial poles to better positions by solving a linear equation (A.8) with known poles, $\{a_m^{(i)}\}$, with i denoting the ith iteration. It can be shown that the zeros of $\sigma(s)$ approach the poles $\{a_m\}$ of $h(s)$, provided that a good approximation of (A.8) exists. The zeros are computed by solving the eigenvalue problem (A.9) with matrices established from the rational model of $\sigma(s)$. By replacing the poles with new poles, a better set of poles is achieved such that

$\{a_m^{(i)}\} \rightarrow \{a_m\}$. Stability of the poles is ensured by flipping any unstable pole into the left half-plane. Finally, the unknown residues are calculated by solving (A.8) with $\sigma(s)$ equal to unity:

$$\overbrace{\left(\sum_{m=1}^{N} \frac{\tilde{r}_m}{s - a_m^{(i)}} + 1\right)}^{\sigma(s)} h(s) \cong \sum_{m=1}^{N} \frac{r_m}{s - a_m^{(i)}} + r_0 \tag{A.8}$$

$$z = eig(\mathbf{A} - \mathbf{b}\mathbf{c}^T) \tag{A.9}$$

In the actual implementation, all poles and residues are forced to be real or to come in complex conjugate pairs.

VF can also be applied to a vector of elements (hence its name), which results in all elements in the vector becoming fitted with a common pole set. By stacking the upper (or lower) triangle of a matrix **H** in a single vector and subjecting it to VF, a symmetrical and stable pole-residue model (A.10) is obtained:

$$\mathbf{H}(s) \cong \sum_{m=1}^{N} \frac{\mathbf{R}_m}{s - a_m} + \mathbf{R}_0 \tag{A.10}$$

Several improvements have been made to the original VF formulation in [10], including:

- relaxation of the non-triviality constraint in order to achieve faster convergence and less biasing [17]
- orthonormalization of basis functions in order to reduce sensitivity to initial poles [18]
- fast implementation [19] when applied to vector of elements
- modal formulation, which maintains the relative accuracy of the eigenvalues of a matrix **H**, via inverse weighting [20].

In addition, VF has been extended for use with responses in the time domain [21] and the z-domain [22].

In this annex we apply a variant of VF, which uses a combination of relaxation and fast implementation – the fast relaxed vector fitting (FRVF).

A.5 Passivity

Although a model extracted by VF has stable poles only, the model may still yield unstable results when included in a time-domain simulation. This is because the model may generate power under certain terminal conditions, since VF does not guarantee the *passivity* of the extracted model. Passivity can, however, be enforced by a post-processing step, as described below.

We will assume that the model is formulated in terms of admittance parameters and a pole-residue model, which defines the relation between terminal voltages **v** and terminal currents **i**,

$$\mathbf{i}(s) = \mathbf{Y}(s)\mathbf{v}(s) \tag{A.11}$$

with

$$\mathbf{Y}(s) = \sum_{m=1}^{N} \frac{\mathbf{R}_m}{s - a_m} + \mathbf{R}_0. \tag{A.12}$$

When the extracted model (A.12) is symmetrical, passivity implies the real part of $\mathbf{Y}$ has positive eigenvalues, that is,

$$eig(\mathrm{Re}\{\mathbf{Y}(s)\}) > 0. \tag{A.13}$$

The passivity can be enforced [11] by perturbing the residues of the model while minimizing the change to its behaviour (A.14a), such that the passivity condition (A.14b) is satisfied:

$$\mathbf{\Delta Y} = \sum_{m=1}^{N} \frac{\Delta \mathbf{R}_m}{s - a_m} + \Delta \mathbf{R}_0 \cong \mathbf{0} \tag{A.14a}$$

$$eig\left(\mathrm{Re}\left\{\mathbf{Y} + \sum_{m=1}^{N} \frac{\Delta \mathbf{R}_m}{s - a_m} + \Delta \mathbf{R}_0\right\}\right) > 0 \qquad \forall s \tag{A.14b}$$

Equation (A.14a) is cast in the form of a linear problem $\mathbf{A}_{sys}\, \Delta\mathbf{x} \cong 0$, while (A.14b) is formulated as a linear constraint $\mathbf{B}_{sys}\, \Delta\mathbf{x} < \mathbf{c}$ via first-order eigenvalue perturbation [11]. The actual solving of (A.14) [11] can be done using quadratic programming (A.15):

$$\min_{\Delta\mathbf{x}} \frac{1}{2}(\Delta\mathbf{x}^T\, \mathbf{A}_{sys}^T \mathbf{A}_{sys}\, \Delta\mathbf{x}) \tag{A.15a}$$

$$\mathbf{B}_{sys}\, \Delta\mathbf{x} < \mathbf{c} \tag{A.15b}$$

Other passivity enforcement schemes are possible, including perturbation of Hamiltonian matrix eigenvalues with minimization of an energy norm [23]. In this annex we use one version that perturbs the residue matrix eigenvalues (spectral perturbation) in order to reduce the computational effort [24].

A.6 Matrix Fitting Toolbox

A.6.1 General

Some software packages are available that can be used for rational function approximation, such as

- IdEM (Politecnico di Torino, Italy) [25]
- matrix fitting toolbox (SINTEF, Norway) [26].

Many useful tools are also available in the SUMO Lab [27] from the University of Ghent, Belgium.

In this annex we will use routines from the matrix fitting toolbox (MFT). These routines are open-source Matlab functions that can be freely downloaded from the web [26].

A.6.2 Overview

VFdriver.m is a routine for fitting a symmetrical, square matrix $\mathbf{H}$, given at frequencies in array s. The performance of the routine is controlled via a structure *opts*, such as the number of iterations, automated initial pole specification, least-squares weighting (error control) and plotting of results. The extracted model is returned in a structure *SER*, in pole-residue form and in state-space form. The user can request the state-space model to have $\mathbf{A}$ being diagonal with a mix of real and complex conjugate elements, or a real-only model (with 2×2 blocks on the diagonal of $\mathbf{A}$). The actual fitting is done by routine *vectfit3.m*, which is an implementation of the FRVF [10, 17, 19] – see Figure A.2.

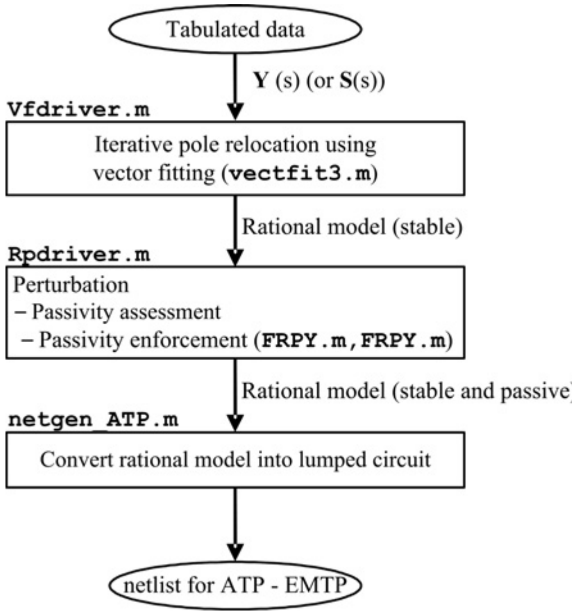

Figure A.2 Computational procedure.

Function call: `[SER,rmserr,Hfit,opts2]=VFdriver(H,s,poles,opts)`

RPdriver.m is a routine for enforcing passivity of a model that has been previously extracted by *VFdriver*. The routine identifies bands of passivity violations and enforces passivity at a set of carefully selected frequencies, so as to enforce passivity while minimizing the change to the original behaviour. The performance of the routine is controlled via a structure *opts*, such as least-squares weighting (error control) and iterations. The passivity assessment is done using a half-size test matrix [28, 29], while the passivity enforcement is done using perturbation of residue matrix eigenvalues [24]. The associated quadratic programming problem (A.15) is solved using the Matlab routine *quadprog.m*, which is part of the Matlab Optimization Toolbox. Note that the routine can be applied to models that represent admittance (or impedance) parameters, as well as scattering (S-) parameters.

Function call: `[SER,Yfit,opts2]=RPdriver(SER,s,opts)`

netgen.m is a routine for converting the model (contained in structure *SER*) into a lumped RLC circuit representation. The RLC network is dumped to a file as an ATP-EMTP netlist.

Function call: `netgen_ATP(SER,NOD,fname)`

A.7 Example A.1: Electrical Circuit

One of the examples included in the MFT is the electrical circuit in Figure A.3. The frequency response is calculated in the range 10 Hz to 100 kHz and is subjected to rational fitting by routine *VFdriver,* using eight pole-residue terms, see (A.10). The fitting error is close to machine precision – see Figure A.4.

The resulting model is exported to a netlist for ATP by routine *netgen_ATP*. A time-domain simulation is carried out where a unit step voltage is applied to terminal 1 in Figure A.3 with terminal 2 grounded – see Figure A.5. The simulated current flowing from ground into terminal 2 is shown in Figure A.6, along with the analytical solution. Clearly, a very accurate result has been achieved.

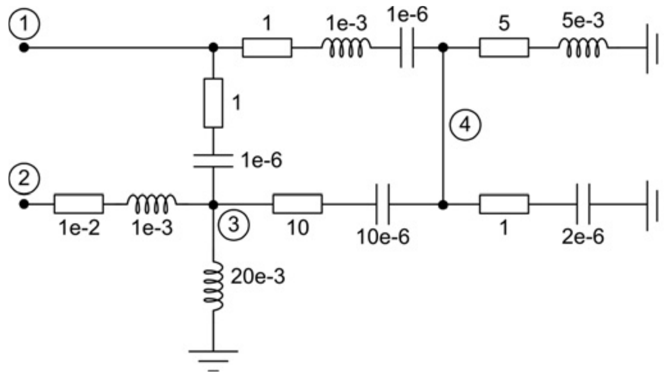

Figure A.3 Lumped circuit. Circuit values in ohms, henries and farada.

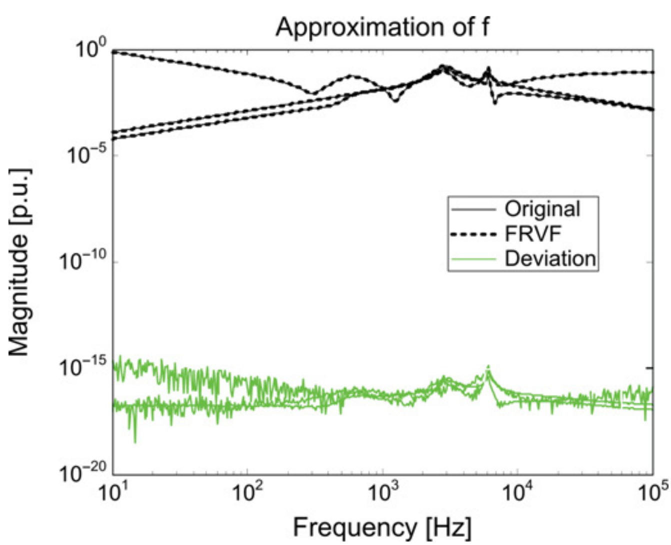

Figure A.4 Rational fitting of **Y**.

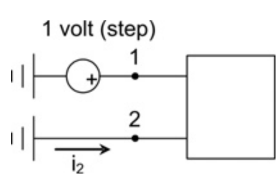

Figure A.5 Step voltage excitation on terminal 1.

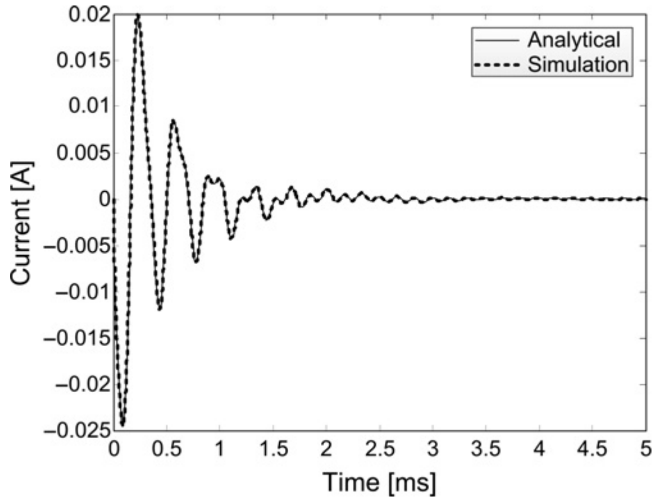

Figure A.6 Current response on terminal 2. ATP simulation vs analytical solution.

A.8 Example 6.2: High-Frequency Transformer Modelling

A.8.1 Measurement

This example is taken from wideband modelling of power transformers from frequency sweep measurements. The transformer is a 300 kVA distribution transformer with 11 kV/230 V voltage ratio – see Figure A.7. Using a measurement setup similar to the one in [9], the 6×6 admittance matrix $\mathbf{Y}$ has been measured in the range 50 Hz to 10 MHz.

A.8.2 Rational Approximation

Using the routine *VFdriver*, a rational model (A.10) with 80 pole-residue terms is extracted. The call requests stable poles only, 10 iterations, and inverse magnitude weighting for achieving relative error control. Total computation time: 9 sec. Figure A.8 shows that a highly accurate fitting result is achieved over the full frequency band.

A.8.3 Passivity Enforcement

The model is passed to routine *RPdriver,* in order to enforce passivity of the model. The function call requests inverse weighting for the least-squares part of the problem (A.15a). Two iterations are used for the inner loop of the iterative procedure. After a total of 13 sec, a passive model is returned. Figure A.9 shows that the passivity enforcement step removes a large passivity violation above 10 MHz; that is, all eigenvalues of $\mathbf{G} = \mathrm{Re}\{\mathbf{Y}\}$ are enforced to be positive.

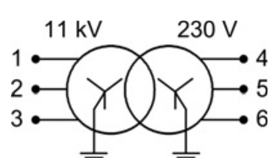

Figure A.7 Distribution transformer.

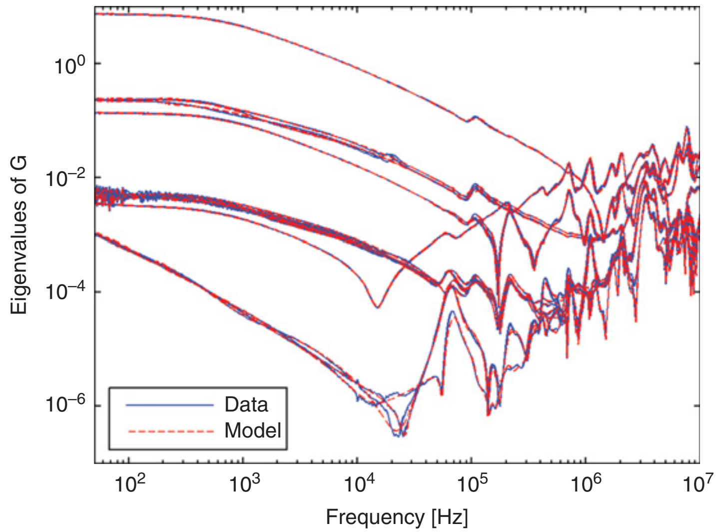

Figure A.8 Rational approximation. Elements of **Y**.

A.8.4 Time-Domain Simulation

Using routine *netgen_ATP*, a lumped circuit equivalent is generated for use with ATP-EMTP. Using ATP, the voltage step response on terminals 4 and 6 is simulated for the terminal conditions in Figure A.10. The voltage waveforms are shown in Figure A.11, together with the simulated response using recursive convolution [2]. The simulation based on recursive convolution was done in a small Matlab program, assuming trapezoidal integration [12, 30]. The two approaches give a nearly identical result. (The difference between the traces is smaller than $1E-5$).

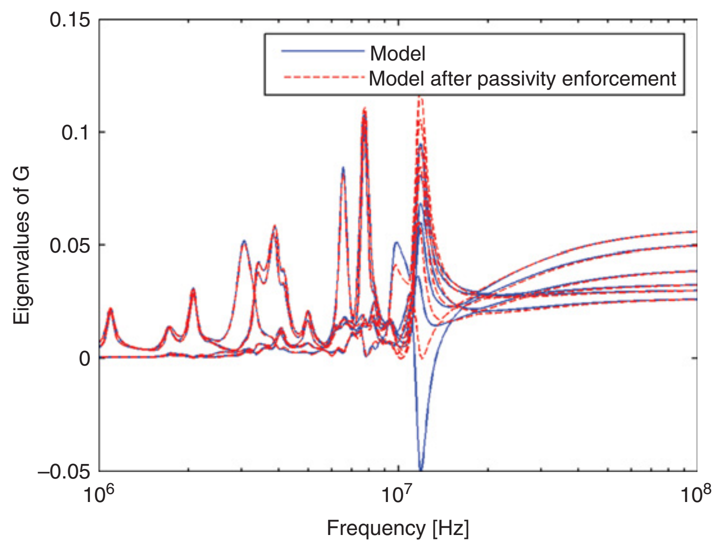

Figure A.9 Passivity enforcement. Eigenvalues of **G**.

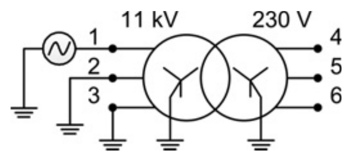

Figure A.10 Step voltage excitation.

A.8.5 Comparison with Time-Domain Measurement

As a validation of the measurement and modelling procedure, we compare measured and simulated time-domain waveforms for the excitation in Figure A.10. The measured step voltage excitation on terminal 1 is realized in the simulation (Matlab program with recursive convolution) as an ideal voltage source, and the voltage response at terminals 4 and 6 are simulated and compared with the measurement. Figure A.12 shows that an excellent agreement is achieved. (The dots represent a fraction of the time-steps).

Figure A.13 shows the same result as in Figure A.12, when the passivity enforcement step has not been carried out. It is seen that the simulation becomes unstable. Thus, passivity enforcement is a mandatory step in the modelling procedure.

In [31], the extracted model was applied in a number of study cases which demonstrated that a transient overvoltage on a feeder cable could lead to excessive overvoltages due to resonance between the cable and the transformer.

Figure A.14 shows the diagram of one case. Two cables of equal length are connected to a busbar that is fed from an overhead line. When switching in the second cable, an oscillating overvoltage results on the cable due to travelling waves which propagate back and forth between the two cables. The dominant frequency component coincides with a peak in the transformer transfer voltage from high to low. This result in an excessive overvoltage on the LV side, – see Figure A.15.

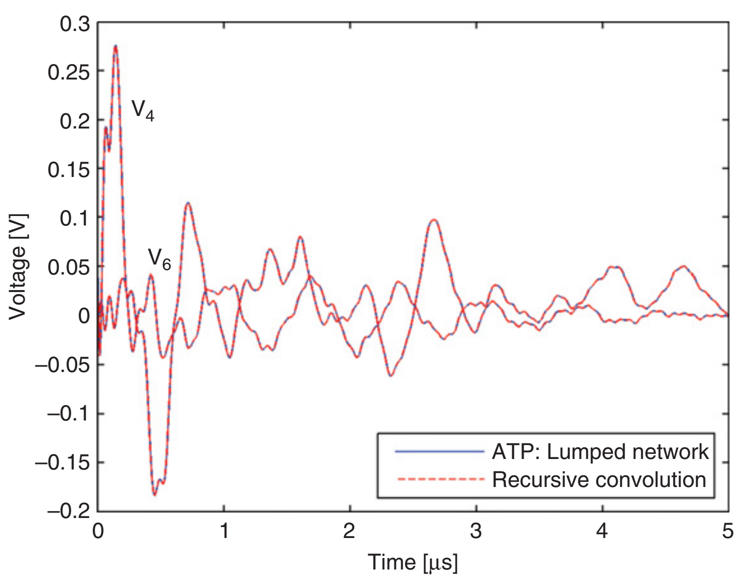

Figure A.11 Step voltage response.

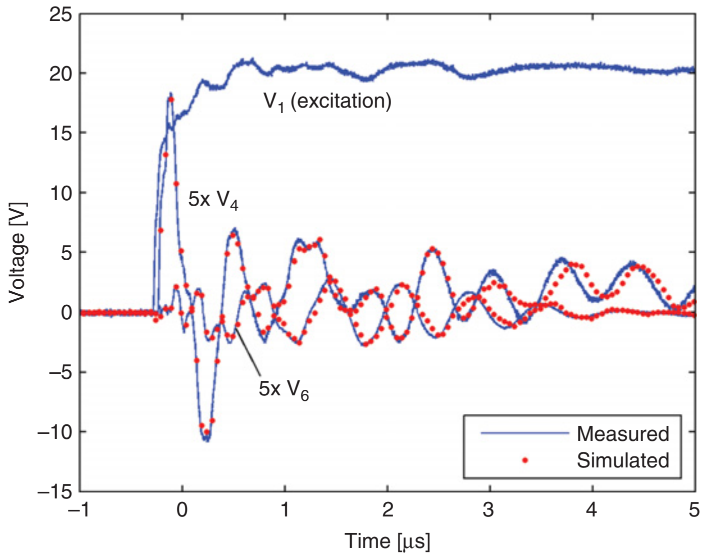

Figure A.12 Simulated vs measured voltage response.

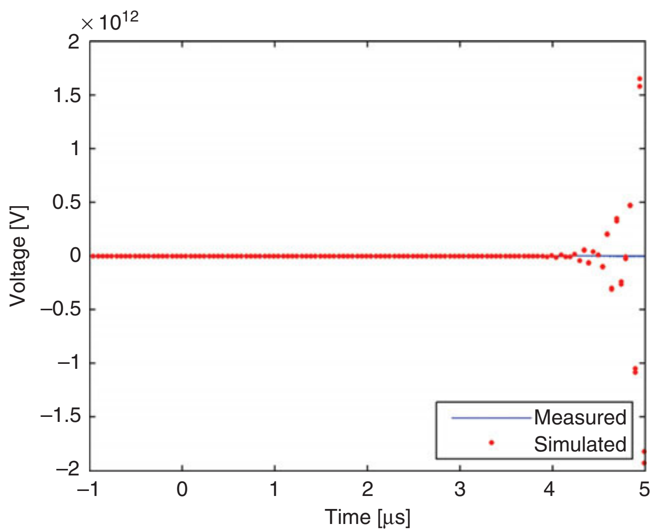

Figure A.13 Simulated vs measured voltage response. No passivity enforcement.

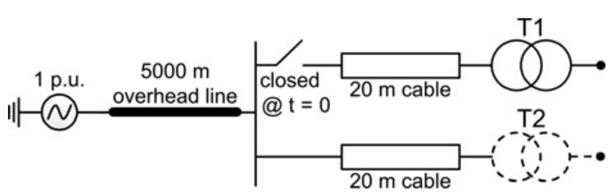

Figure A.14 Transformer energization from three-phase power system. Closing first breaker pole at $t = 0$ [31].

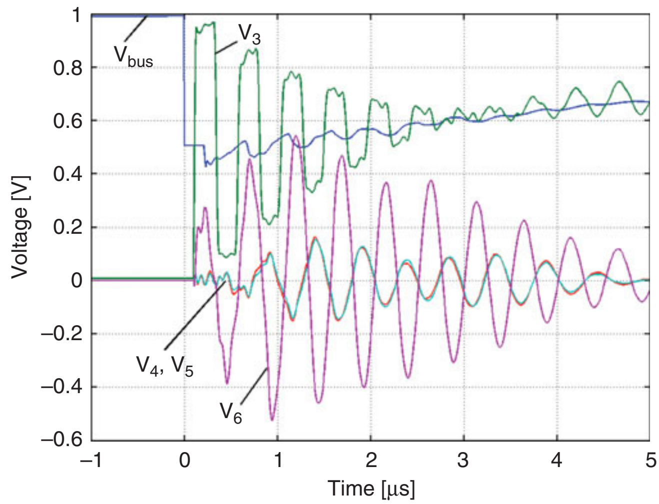

Figure A.15 Transient overvoltages (© 2010 IEEE) [31].

References

[1] Dommel, H.W. (1986) *ElectroMagnetic Transients Program. Reference Manual (EMTP Theory Book)*, Bonneville Power Administration, Portland.

[2] Semlyen, A. and Dabuleanu, A. (1975) Fast and accurate switching transient calculations on transmission lines with ground return using recursive convolutions. *IEEE Transactions on Power Apparatus and Systems*, **94**(2), 561–575.

[3] Martí, J.R. (1982) Accurate modelling of frequency-dependent transmission lines in electromagnetic transient simulations. *IEEE Transactions on Power Apparatus and Systems*, **101**(1), 147–157.

[4] Noda, T., Nagaoka, N., and Ametani, A. (1996) Phase domain modeling of frequency-dependent transmission lines by means of an ARMA model. *IEEE Transactions on Power Delivery*, **11**(1), 401–411.

[5] Morched, A., Gustavsen, B., and Tartibi, M. (1999) A universal model for accurate calculation of electromagnetic transients on overhead lines and underground cables. *IEEE Transactions on Power Delivery*, **14**(3), 1032–1038.

[6] Morched, A., Ottevangers, J., and Martí, L. (1993) Multiport frequency dependent network equivalents for the EMTP. *IEEE Transactions on Power Delivery*, **8**(3), 1402–1412.

[7] Noda, T. (2005) Identification of a multiphase network equivalent for electromagnetic transient calculations using partitioned frequency response. *IEEE Transactions on Power Delivery*, **20**(2), 1134–1142.

[8] Morched, A., Martí, L., and Ottevangers, J. (1993) A high frequency transformer model for the EMTP. *IEEE Transactions on Power Delivery*, **8**(3), 1615–1626.

[9] Gustavsen, B. (2004) Wide band modeling of power transformers. *IEEE Transactions on Power Delivery*, **19**(1), 414–422.

[10] Gustavsen, B. and Semlyen, A. (1999) Rational approximation of frequency domain responses by vector fitting. *IEEE Transactions on Power Delivery*, **14**(3), 1052–1061.

[11] Gustavsen, B. and Semlyen, A. (2001) Enforcing passivity for admittance matrices approximated by rational functions. *IEEE Transactions on Power Systems*, **16**(1), 97–104.

[12] Gustavsen, B. and Mo, O. (2007) Interfacing convolution based linear models to an electromagnetic transients program. International Conference on Power Systems Transients, 4–7 June 2007, Lyon, France.

[13] Gustavsen, B. (2002) Computer code for rational approximation of frequency dependent admittance matrices. *IEEE Transactions on Power Delivery*, **17**(4), 1093–1098.

[14] Sanathanan, C.K. and Koerner, J. (1963) Transfer function synthesis as a ratio of two complex polynomials. *IEEE Transactions on Automatic Control*, **8**(1), 56–58.

[15] Bode, H.W. (1945) *Network Analysis and Feedback Amplifier Design*, D. Van Nostrand, Inc.

[16] Martí, J.R. (1981) The problem of frequency dependence in transmission line modelling. PhD thesis, The University of British Columbia, Canada.

[17] Gustavsen, B. (2006) Improving the pole relocating properties of vector fitting. *IEEE Transactions on Power Delivery*, **21**(3), 1587–1592.

[18] Deschrijver, D., Haegeman, B., and Dhaene, T. (2007) Orthonormal vector fitting: a robust macromodeling tool for rational approximation of frequency domain responses. *IEEE Transactions on Advanced Packaging*, **30**(2), 216–225.

[19] Deschrijver, D., Mrozowski, M., Dhaene, T., and De Zutter, D. (2008) Macromodeling of multiport systems using a fast implementation of the vector fitting method. *IEEE Microwave and Wireless Components Letters*, **18**(6), 383–385.

[20] Gustavsen, B. and Heitz, C. (2009) Fast realization of the modal vector fitting method for rational modeling with accurate representation of small eigenvalues. *IEEE Transactions on Power Delivery*, **24**(3), 1396–1405.

[21] Grivet-Talocia, S. (2003) Package macromodeling via time-domain vector fitting. *IEEE Microwave and Wireless Components Letters*, **13**(11), 472–474.

[22] Mekonnen, Y.S. and Schutt-Aine, J.E. (2007) Broadband macromodeling of sampled frequency data using z-domain vector-fitting method. Proceedings of IEEE Workshop on Signal Propagation on Interconnects, Genova, Italy, 13–16 May 2007, pp. 45–48.

[23] Grivet-Talocia, S. (2004) Passivity enforcement via perturbation of Hamiltonian matrices. *IEEE Transactions on Circuits and Systems I*, **51**(9), 1755–1769.

[24] Gustavsen, B. (2008) Fast passivity enforcement for pole-residue models by perturbation of residue matrix eigenvalues. *IEEE Transactions on Power Delivery*, **23**(4), 2278–2285.

[25] IdEM website, http://www.emc.polito.it/software/IdEM/idem_home.asp.

[26] Vector Fitting website, http://www.sintef.no/Projectweb/VECTFIT/.

[27] SUMO Lab website, http://www.sumo.intec.ugent.be/.

[28] Semlyen, A. and Gustavsen, B. (2009) A half-size singularity test matrix for fast and reliable passivity assessment of rational models. *IEEE Transactions on Power Delivery*, **24**(1), 345–351.

[29] Gustavsen, B. and Semlyen, A. (2009) On passivity tests for unsymmetrical models. *IEEE Transactions on Power Delivery*, **24**(3), 1739–1741.

[30] Gustavsen, B. and De Silva, H.M.J. (2013) Inclusion of rational models in and electromagnetic transients program – Y-parameters, Z-parameters, S-parameters, transfer functions. *IEEE Transactions on Power Delivery*, **28**(2), 1164–1174.

[31] Gustavsen, B. (2010) Study of transformer resonant overvoltages caused by cable-transformer high-frequency interaction. *IEEE Transactions on Power Delivery*, **25**(2), 770–779.